

High-Performance Negative Differential Resistance Behavior in Fullerenes Encapsulated Double-Walled Carbon Nanotubes

著者	Li Y. F., Kaneko T., Hatakeyama R.
journal or publication title	Journal of Applied Physics
volume	106
number	12
page range	124316
year	2009
URL	http://hdl.handle.net/10097/52044

doi: 10.1063/1.3273496

High-performance negative differential resistance behavior in fullerenes encapsulated double-walled carbon nanotubes

Y. F. Li,^{a)} T. Kaneko, and R. Hatakeyama

Department of Electronic Engineering, Tohoku University, Sendai 980-8579, Japan

(Received 17 September 2009; accepted 18 November 2009; published online 29 December 2009)

The authors report negative differential resistance (NDR) characteristics observed in nanodevices constructed using three types of fullerenes (C_{60} , C_{70} , and C_{84}) encapsulated metallic double-walled carbon nanotubes. The NDR behavior persists from room temperature (300 K) to lower temperatures, and a significantly high on-off peak-to-valley current ratio is observed for many of the devices examined. The fullerene species exerts a strong influence on the peak voltage of the NDR, which exhibits a linear decrease with increasing fullerene size. The observed current-voltage curves are highly reproducible during measurements, and fully reversible upon change in the bias sweep direction. In addition, the peak current of the NDR is found to increase significantly under light illumination and is recoverable in the absence of light, which indicates potential for applications such as logic optoelectronic devices. © 2009 American Institute of Physics.

[doi:10.1063/1.3273496]

I. INTRODUCTION

The discovery of negative differential resistance (NDR) in semiconductors was a significant event in device physics.¹ The presence of NDR is a useful feature that has a wide variety of circuit applications, such as high-speed switches, high-frequency oscillators, amplifiers, and logic. Over the past three decades, a large number of NDR devices have been fabricated based on the GaAs–AlGaAs superlattice structure, which exhibits resonance-tunneling characteristics. Recently, many research groups have explored other types of material systems, such as nanoscale molecular junctions,² Si quantum dot structures,³ and Te-filled zeolites,⁴ to improve device performance. Although NDR devices employing different materials have been realized, fabrication with high peak-to-valley current ratio (PVCR) and good reproducibility remains a significant challenge. In addition, the scaling of NDR devices designs down to increasingly smaller sizes is rapidly approaching the fundamental limits, and new devices based on nanotechnology will begin to be substituted for conventional systems. In recent years, carbon nanotubes (CNTs) have become attractive candidates for nanoelectronic applications, due to their small size, unique structure, and outstanding electronic properties. A number of nanodevices based on various types of CNTs, including single-electron transistors,⁵ field-effect transistors⁶ and rectifying diodes⁷ have been reported. In particular, double-walled CNTs (DWNTs), consisting of two concentric cylindrical graphene layers, have attracted increasing interest because of advantages over other types of CNTs, such as their size and electrical and mechanical properties.⁸ Tunnel barriers, quantum dot, or quantum well structures can be easily implemented in the nanospace of DWNTs by means of built-in heterostructures, such as encapsulation of other foreign atoms or molecules within the DWNTs. On the other hand, fullerene mol-

ecules, such as C_{60} , with spherical shape and unique electronic structure, are already of physical interest for studies on low-dimensional electron systems.^{9–11} In this sense, numerous fullerenes encapsulated in one-dimensional (1D) DWNTs may provide an ideal superlattice heterostructure for the testing of quantum mechanical effects.

Here, we report the electrical transport properties of nanodevices fabricated with fullerenes (C_{60} , C_{70} , and C_{84}) encapsulated metallic DWNTs (fullerene@DWNTs). The most attractive feature of the devices is that they exhibit reproducible NDR characteristics as a result of their strong resonance tunneling effect. Typical NDR of the devices yields a high PVCR, up to approximately 10^4 at room temperature, which enables the devices to be easily switched on and off. Peak voltages of NDR are found to be strongly dependent on the size of the fullerenes and display a linear downshift with an increase in the size of the encapsulated fullerenes. Further measurements indicate that the NDR behavior is optically controllable at room temperature, and the switching characteristics are reversible in the absence of light. The findings indicate that confined electrons can be sensed via light.

II. EXPERIMENTAL DETAILS

A. Synthesis and characterization of various fullerene@DWNTs

Raw DWNTs were prepared by arc discharge using Fe as a catalyst, followed by a purification process to remove the catalyst and amorphous carbon. Air oxidation was carried out at 733 K for 30 min to open the DWNTs prior to encapsulation of the fullerenes. Encapsulation of C_{60} , C_{70} , and C_{84} fullerenes inside DWNTs was realized using a vapor diffusion or plasma-ion irradiation method, similar to that for the encapsulation of fullerenes inside single-walled CNTs (SWNTs).¹² The fullerene@DWNT samples obtained during the encapsulation process were then purified in toluene to remove the excess fullerene molecules attached to the

^{a)}Author to whom correspondence should be addressed. Electronic mail: yfli@plasma.ecei.tohoku.ac.jp. FAX: +81-022-263-9225.

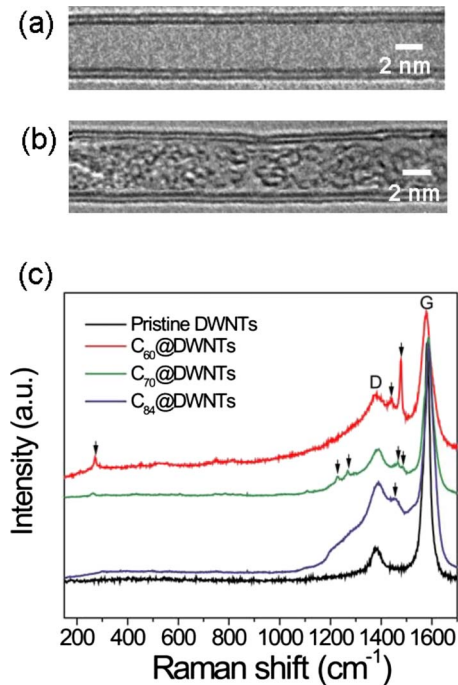


FIG. 1. (Color online) (a) TEM image of an empty DWNT with inner and outer diameters of 4.0 and 4.8 nm, respectively. (b) TEM image of C_{60} @DWNT. (c) Raman spectra of pristine DWNTs, and C_{60} -, C_{70} -, and C_{84} fullerene@DWNTs.

surface of the DWNTs. Transmission electron microscopy (TEM, Hitachi HF-2000) operated at 200 kV and micro-Raman scattering spectroscopy with an Ar laser at 488 nm were used for characterization of the samples.

B. Electrical transport measurements

The electrical transport properties of the various fullerene@DWNTs were measured by constructing field-effect transistors (FETs) with the fullerene@DWNTs as the current channels. An individual nanotube bridging the source and drain electrodes was identified by atomic force microscopy (AFM). We have previously reported experimental details for the fabrication of FET devices using various kinds of CNTs.¹³ The electrical transport properties were measured from the source-drain current I_{DS} , as a function of the source-drain voltage V_{DS} , or gate bias V_G . Electrical measurements were carried using a semiconductor parameter analyzer (Agilent 4155C) under both dark conditions and under light illumination in a vacuum (10^{-4} – 10^{-5} Pa). Light-induced switching transport measurements were performed under exposure to light with wavelengths in the range of 390–1100 nm with illumination intensity <50 mW/cm² generated by a 150 W Xe lamp (LSX-2501).

III. RESULTS AND DISCUSSION

A. TEM and Raman spectroscopy characterization

A TEM image of an empty DWNT with inner and outer diameters of approximately 4.0 and 4.8 nm, respectively, is shown in Fig. 1(a). In contrast, Fig. 1(b) presents a typical TEM image of a DWNT filled with numerous C_{60} molecules. In this case, the encapsulation ratio of fullerenes inside

DWNTs (encapsulation DWNTs/total DWNTs) was more than 80% according to TEM observations. Only an amorphous phase of C_{60} molecules was identified inside the DWNT, due to the large inner diameter of the DWNT of approximately 4.5 nm because the packing arrangement of C_{60} is very sensitive to the nanotube diameter, which is in agreement with that previously reported.¹⁴ Similarly, amorphous C_{70} or C_{84} molecules have also been observed inside DWNTs.

The Raman spectra shown in Fig. 1(c) further confirmed that various fullerene (C_{60} , C_{70} , and C_{84}) molecules were encapsulated within the DWNTs, according to the two typical D-band and G-band peaks observed at 1378 and 1584 cm^{-1} , respectively. However, the radial breathing mode was not detected in any of the nanotube samples, due to the larger diameter of the DWNTs. However, significant signal changes, indicated by arrows in Fig. 1(c), can be recognized in the Raman spectra for the three different DWNT-encapsulated fullerenes, when compared with that for the pristine DWNTs. In the case of C_{60} -filled DWNTs, a strong peak at 1476 cm^{-1} , corresponding to intermolecular Raman active frequency (tangential mode) $Ag(2)$ of C_{60} , is clearly observed due to C_{60} encapsulation. The weak peak at 1437 cm^{-1} near the D-band can be attributed to the $Hg(7)$ mode of C_{60} molecules. Another weak peak is also detected at a low frequency of 271 cm^{-1} , which corresponds to the $Hg(1)$ mode of C_{60} , which may suggest the formation of dimers or clusters because a large amount of C_{60} molecules can be filled inside DWNTs as indicated by the TEM observations. For C_{70} -filled DWNTs, the change in the Raman signals can be assigned as follows according to Refs. 15–17; 1228 cm^{-1} (A'_1, E''_1, E'_2), 1268 cm^{-1} (E''_1, E'_2), 1464 cm^{-1} (A'_1, E''_1, E'_2), and 1484 cm^{-1} (A'_1, E'_1), which is different from the case of C_{60} -filled DWNTs. Furthermore, after C_{84} encapsulation, a large signal change is distinguished in the region between the D-band and Ag mode (1458 cm^{-1}), where the Raman spectrum becomes broad and asymmetric. Therefore, the Raman characterization provides evidence that the different fullerenes (C_{60} , C_{70} , and C_{84}) have been encapsulated inside DWNTs.

B. Comparison of NDR behavior observed in different fullerene@DWNTs

Figures 2(a)–2(c) show I_{DS} - V_{DS} curves measured at a gate voltage of $V_G=0$ V for three independent nano-devices that were fabricated using C_{60} , C_{70} , and C_{84} fullerene@DWNTs, respectively. The inset of Fig. 2(a) shows an AFM image of the FET device with one C_{60} @DWNT as the current channel. Compared with the typical linear behavior of pristine metallic DWNT, the observed I_{DS} - V_{DS} curve shown in Fig. 2(a) for the C_{60} @DWNT device exhibits strong NDR characteristics at a positive bias of 6.6 V and a negative bias of -6.9 V. The initial increase in current is followed by a sharp decrease, rather than the linear increase expected from Ohm's law, when the voltage is more than the absolute value of approximately 7 V. Unlike previously reported devices, where S- or N-shaped NDR characteristics are usually observed, this

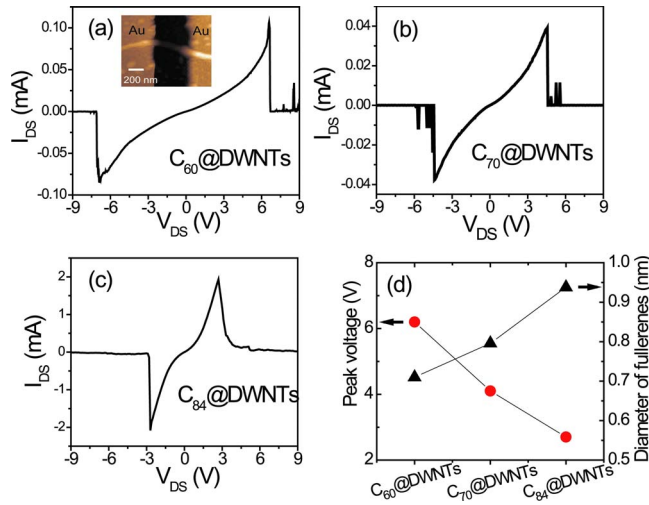


FIG. 2. (Color online) Characteristic I_{DS} - V_{DS} curves ($V_G=0$ V) for (a) C_{60} @DWNT, (b) C_{70} @DWNT, and (c) C_{84} @DWNT devices measured at room temperature. The inset in (a) shows an AFM image of a C_{60} @DWNT-FET device. (d) Average peak voltages of NDR for C_{60} @DWNT, C_{70} @DWNT, and C_{84} @DWNT devices showing a linear decrease with increasing fullerene diameter.

device exhibits strong NDR at room temperature. In the off region, the valley current is reduced to the level of approximately 10^{-4} mA. Despite the difference in the peak position, robust and sharp NDR characteristics were also found for the device constructed with a C_{70} @DWNT, as shown in Fig. 2(b), where a high PVCN of approximately 10^4 was symmetrically observed at 4.5 and -4.3 V with a cutoff current in the order of 10^{-4} μ A. The PVCN serves as a figure of merit for resonance tunneling devices; therefore, the intrinsic device characteristics observed in this study are much better than those reported for conventional solid-state quantum well resonance tunneling heterostructures.^{18,19} In addition to the large PVCN, all the NDR devices were found to exhibit large peak currents, and the maximum value was typically several orders of magnitude larger than the currents measured for pristine DWNTs at the same corresponding bias, in which no NDR behavior is observed. Figure 2(c) shows the I_{DS} - V_{DS} characteristics of the C_{84} @DWNT device, in which the maximum peak current of NDR reached an unusually high value of approximately 1.93 mA at a positive bias of 2.7 V and 2.09 mA at a negative bias of -2.7 V. According to these observations, it can be concluded that the NDR behavior in the DWNTs is completely dependent on fullerene encapsulation. It is also interesting to mention that the peak positions of NDR move toward lower voltages with increasing diameter of the encapsulated fullerenes, as indicated in Fig. 2(d), in which the average peak voltages (V_p) for the C_{60} @DWNT, C_{70} @DWNT, and C_{84} @DWNT devices were 6.1, 4.1, and 2.7 V, respectively, based on measurements for more than 15 devices of each fullerene@DWNT type.

The notable difference between the present devices and conventional ones is that the NDR characteristics are fully reversible in accordance with the change in the bias sweep direction or rate, and as a result, clear hysteresis loops are rarely observed during the entire measurement. For a given

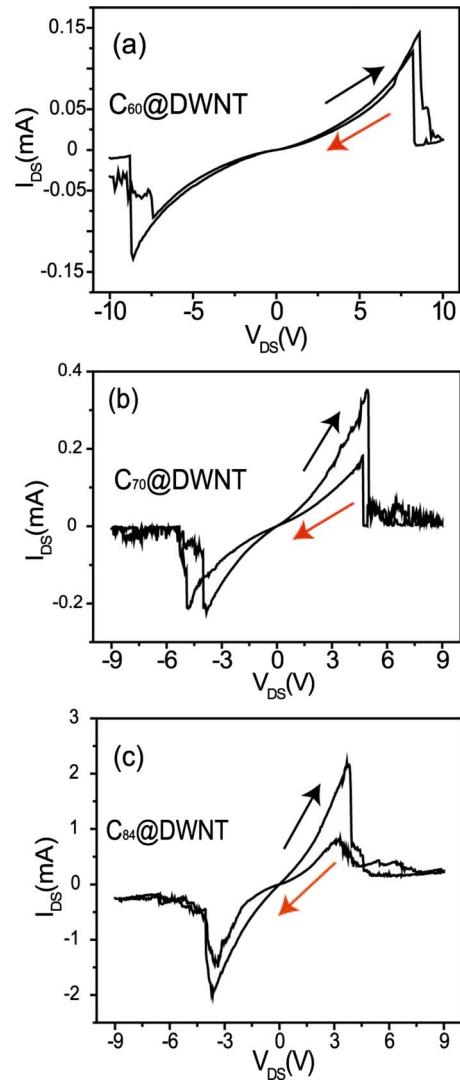


FIG. 3. (Color online) I_{DS} - V_{DS} curves measured under forward and backward voltage sweeps for (a) C_{60} @DWNT, (b) C_{70} @DWNT, and (c) C_{84} @DWNT devices at room temperature (300 K).

device only fluctuations in peak position and peak current are recognized, regardless of the type of scan performed, as seen in Fig. 3(a), in which clear NDR regions are observed for the C_{60} @DWNT at 6.8 and -7.3 V in consecutive forward and backward voltage sweeps. Such reproducible NDR characteristics were also identified in the devices fabricated with C_{70} @DWNTs and C_{84} @DWNTs, as shown in Figs. 3(b) and 3(c), respectively, which indicates that their performance is superior to that for most conventional devices, in which limited reproducibility of the NDR behavior mainly appears during the forward sweep.^{3,4,20}

C. Temperature-dependence of NDR behavior in fullerene@DWNTs

Another attractive feature of the present devices is that the NDR characteristic is observed at room temperature and lower, as indicated by the I_{DS} - V_{DS} curves measured for the C_{84} @DWNT device in the temperature range of 10–300 K [Fig. 4(a)]. It is noted that the current of the device exhibits a monotonic decrease with the decrease in temperature.

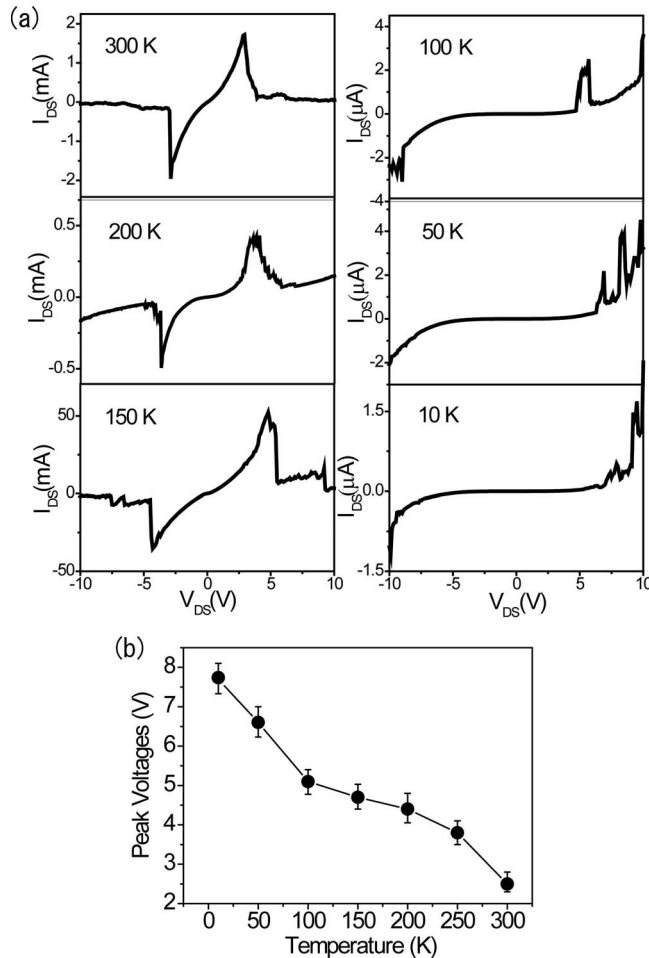


FIG. 4. (a) I_{DS} - V_{DS} curves of a C_{84} @DWNT device with NDR behavior measured in the temperature range from 300 to 10 K. (b) Peak voltages of NDR indicate an increase with decreasing temperature.

There are two possible reasons for the observed phenomenon. One is the typical reduction in thermal conductance for nanotubes with decreasing temperature, as described elsewhere,²¹ and the other is the possibility that the coherent transport of electrons in the superlattice structure of the C_{84} @DWNT device may be suppressed at low temperatures, which is considered to diminish the resonance tunneling current. As a result, the PVCRC appears to decrease when the temperature is lower than 150 K, and only small PVCRC values (approximately 10) are observed below 100 K. Moreover, it is found that the peak position shifts to larger V_p with decreasing temperature, as shown in Fig. 4(b). This temperature dependent behavior is similar to that observed for previously reported devices that employ organic molecules to form the active region.² However, after the device was heated to room temperature and measured again, high peak current and PVCRC were again observed, which indicates a rapid recovery of the NDR characteristics.

A possible physical explanation for the observed NDR phenomenon is that a quantum dot superlattice structure is formed in the DWNT after fullerene encapsulation in the large 1D inner space. In contrast, no such NDR behavior has been observed in fullerenes encapsulated SWNTs with diameters of 1.4–1.6 nm, which suggests that DWNTs with large

diameter play an important role in the NDR phenomenon. When the current flows through the nanostructure of fullerene@DWNTs, many current paths exist in one device and numerous fullerene molecules are involved in each path, which results in the capability of carrying a large current at low bias. This is evident from the measured conductance of the NDR device shown in Fig. 2(c), which reaches $-128G_0$ at -2.7 V. This is much larger than the $2G_0$ limitation reported for a perfectly contacting CNT,^{22–24} where $G_0 = 2e^2/h$ is the conductance unit and its value is $77.6 \mu S$ (h : Plank's constant). Thus, it is clear that fullerene molecules participate in the ballistic transport of electrons in multiple conductance channels. When electrons tunnel through such a superlattice structure of fullerene@DWNTs, the coherent nature of ballistic electron propagation can generate constructive interference, which leads to the occurrence of resonance tunneling. With increasing bias voltage, the current increases rapidly, due to an increase in multitunneling paths for electrons. The peak current will appear when the Fermi level of the electrodes matches the formed resonant energy level E_T of the fullerenes. If the bias increases to a value somewhat larger than V_p , at which the Fermi level of the electrodes becomes higher than E_T , the current can suddenly be suppressed, thus causing NDR. In the present study, a sharp reduction in current is also possible due to the occurrence of a strong charging effect, in which electrons trapped on fullerene molecules may screen the applied field and prevent current flow, resulting in the observed sharp NDR. The close dependence of the energy levels on the fullerene size appears to be similar to that for electrons trapped in quantum wells, in which the energy levels and energy spacing between adjacent energy levels of electrons are inversely proportional to the width of the quantum wells. The relationship between the energy levels and the width of an infinite quantum well is given by $E_n = \hbar^2/2m_e (n\pi/L_w)^2$, where $n=1, 2, \dots$, L_w is the width of the quantum well, m_e is the effective mass of the electron, and n is the quantum number associated with the n th energy level of E_n . Considering this, it can be easily envisaged that an analogous effect of fullerene size (<1 nm) on the discrete energy levels of trapped electrons on fullerenes takes place, which may lead to a resultant resonant energy level E_T and related switching voltage V_p that are inversely proportional to the fullerene size.

D. Photoinduced NDR behavior of fullerene@DWNTs

Figure 5(a) presents typical I_{DS} - V_{DS} characteristics of a C_{60} @DWNT-FET device measured with and without light at room temperature. Under light illumination, the current peak (I_p) of NDR exhibits a significant increase from 0.2 to 0.6 mA, and the peak position is shifted from 4.1 V to a lower bias voltage of 3.5 V, due to the reduced tunneling resistance. Apart from the large photoinduced current peak, the PVCRC (I_p/I_V) is found to increase under light illumination. This phenomenon is attributed to the photoinduced neutralization of charge in the quantum dots (or quantum well) by an accumulation of photogenerated holes, which may lead to a lowering of the height of the tunneling barrier related to the dark response. To further elucidate this behavior, the

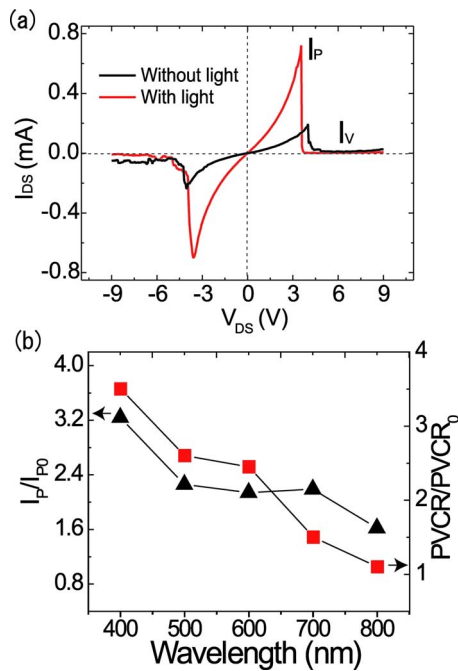


FIG. 5. (Color online) (a) I_{DS} - V_{DS} curves measured with $V_G=0$ V at room temperature for a C_{60} @DWNT with and without light illumination (390 nm). (b) I_P/I_{P0} and $PVCR/PVCR_0$ measured as a function of wavelength, indicating a decrease in the photoinduced current and PVCR with increasing wavelength.

dependence of the photoinduced NDR characteristics on the wavelength of light was investigated. Figure 5(b) shows the ratio of peak current I_P and the PVCR enhanced by light to the original current I_{P0} (I_P/I_{P0}) and $PVCR_0$ ($PVCR/PVCR_0$), respectively, as a function of wavelength. The change in the photoinduced peak current becomes less pronounced with increasing wavelength, the same tendency of which is observed for the value of PVCR. This implies that the main effect of light energy is on the number of holes generated by photons. Measurements made on more than 20 independent devices revealed similar tendencies of wavelength dependence, although not identical. Interestingly, such optically controlled NDR is also found for other fullerenes such as C_{70} and C_{84} encapsulated in DWNTs. The conductance state of the NDR device is entirely reversible when the light is switched on and off, and this behavior is reproducible for multiple cycles. Time resolved measurements were also conducted for the samples in order to further specify the light response transport phenomenon, as shown in Fig. 6, where the I_{DS} at $V_G=0$ V and $V_{DS}=3$ V was measured as a function of time. Compared with the dark characteristics, the peak current of NDR was significantly increased, and the value was more than twice as large as that measured without illumination. When the light source was switched off, the current almost returned to its initial operating state with a lower value.

The sharp NDR behavior is also due to the transient current induced from the charging effect, in which electrons trapped in quantum wells (fullerenes) can screen the applied field, thereby preventing current flow. In this case, oscillation peaks resulting from a Coulomb blockade (CB) are clearly observed in the room temperature I_{DS} - V_G curves, as shown in

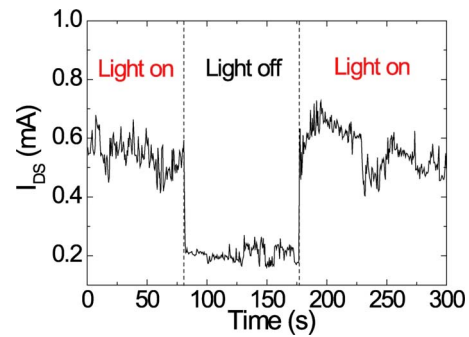


FIG. 6. (Color online) I_{DS} characteristics measured as a function of time with and without light illumination (390 nm) for a C_{60} @DWNT-FET device at $V_G=0$ V and $V_{DS}=3$ V.

Fig. 7, which implies that the charge on the nanotube is quantized, and charging and discharging are not continuous. In other words, the CB in this case leads to a single-electron tunneling phenomenon, due to the strong charging effect in C_{60} encapsulated DWNTs, which agrees with the result shown in Fig. 5(a), where the current is blocked with a V_{DS} larger than 4.5 V. The average gate voltage period ΔV_G between adjacent oscillation peaks is 2.2 V in the absence of light, as seen in Fig. 7(a). However, ΔV_G becomes much larger and periodic (6.0 V) under 390 nm light, as shown in Fig. 7(b), which implies that the capacitance C of the quantum dots (or quantum well) becomes lower under illumination according to $C=e/\Delta V_G$. Consequently, the charging energy $E_c=e^2/2C$ (Ref. 25) of the NDR device becomes higher, in contrast to that without illumination. These results can possibly be attributed to the trapping and accumulation

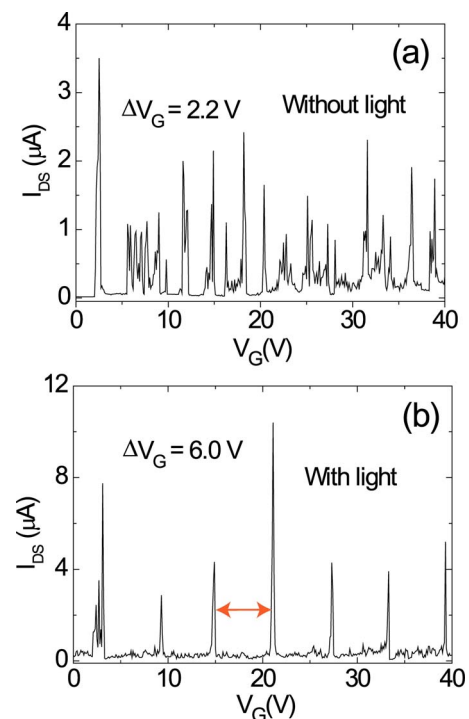


FIG. 7. (Color online) I_{DS} - V_G curves of a C_{60} @DWNT-FET device measured at (a) $V_{DS}=6$ V without light, showing Coulomb oscillation behavior with gate period voltage $\Delta V_G=2.2$ V and (b) under 390 nm light illumination, where ΔV_G is 6.0 V.

of electrons on C₆₀ fullerenes; redox chemistry studies have revealed the ability of fullerenes to accommodate up to six electrons.^{26,27} In the presence of light, the optical and electronic properties of fullerenes are considered to undergo a dramatic change. The oxidation potential of a fullerene in the excited state (C₆₀^{*}, 0.1 V) is much lower than that of C₆₀ in the ground state (2.15 V),²⁸ and as a result, the electron drawing ability of the fullerene is reduced, which can then result in the observed photoinduced CB behavior.

IV. CONCLUSION

The electrical transport properties of three different fullerenes encapsulated metallic DWNTs were measured. In contrast to the empty metallic DWNTs, unique NDR is clearly observed as the result of strong resonance tunneling in the superlattice heterostructure of the fullerene@DWNTs. The peak voltages of NDR are strongly dependent on the type of fullerene, and exhibit a linear decrease with increasing fullerene diameter. The NDR characteristics are reversible, in accordance with variations in the bias sweep direction, and are stable during measurements performed from room temperature to lower temperatures. Under light illumination, the optically controlled NDR phenomenon was observed in the fullerene@DWNTs. The resonance tunneling effect is optically enhanced and the peak current is significantly increased when the device is illuminated. The photoinduced NDR characteristic is strongly dependent on the wavelength. Moreover, a remarkable effect of illumination on the single-electron tunneling phenomenon was observed, which suggests that it is possible to detect the loss or capture of electrons in quantum dots. Further optimization of this effect could be useful for application requiring the detection of a single-electron.

ACKNOWLEDGMENTS

We are grateful to Professor K. Tohji and Mr. K. Motomiya for their assistance with TEM observations. This work was partly performed at the Laboratory for Nanoelectronics and Spintronics, Research Institute of Electrical Communication, Tohoku University. This work was supported by a Grant-in-Aid for Scientific Research from the Ministry of

Education, Culture, Sports, Science and Technology, Japan, JSPS-CAS Core-University Program on Plasma and Nuclear Fusion.

- ¹L. Esaki, *Phys. Rev.* **109**, 603 (1958).
- ²J. Chen, M. A. Reed, A. M. Rawlett, and J. M. Tour, *Science* **286**, 1550 (1999).
- ³N. M. Park, S. H. Kim, S. Maeng, and S. J. Park, *Appl. Phys. Lett.* **89**, 153117 (2006).
- ⁴Z. K. Tang and X. R. Wang, *Appl. Phys. Lett.* **68**, 3449 (1996).
- ⁵S. J. Tans, A. R. M. Verschueren, and C. Dekker, *Nature (London)* **393**, 49 (1998).
- ⁶H. W. Ch. Postma, T. Teepen, Z. Yao, M. Grifoni, and C. Dekker, *Science* **293**, 76 (2001).
- ⁷J. Kong, N. R. Franklin, C. Zhou, M. G. Chapline, S. Peng, K. Cho, and H. Dai, *Science* **287**, 622 (2000).
- ⁸R. Saito, R. Matsuo, T. Kimura, G. Dresselhaus, and M. S. Dresselhaus, *Chem. Phys. Lett.* **348**, 187 (2001).
- ⁹H. Park, J. Park, A. K. L. Lim, E. H. Anderson, A. P. Alivisatos, and P. L. McEuen, *Nature (London)* **407**, 57 (2000).
- ¹⁰H. S. Majumdar, J. K. Baral, R. Österbacka, O. Ikkala, and H. Stubb, *Org. Electron.* **6**, 188 (2005).
- ¹¹S. Paul, A. Kanwal, and M. Chhowalla, *Nanotechnology* **17**, 145 (2006).
- ¹²Y. F. Li, T. Kaneko, and R. Hatakeyama, *Nanotechnology* **19**, 415201 (2008).
- ¹³Y. F. Li, R. Hatakeyama, T. Kaneko, T. Izumida, T. Okada, and T. Kato, *Nanotechnology* **17**, 4143 (2006).
- ¹⁴A. N. Khlobystov, D. A. Britz, A. Ardavan, and G. A. D. Briggs, *Phys. Rev. Lett.* **92**, 245507 (2004).
- ¹⁵V. Schettino, M. Pagliai, and G. Cardini, *J. Phys. Chem. A* **106**, 1815 (2002).
- ¹⁶S. H. Gallagher, R. S. Armstrong, R. D. Bolskar, P. A. Lay, and C. Reed, *J. Am. Chem. Soc.* **119**, 4263 (1997).
- ¹⁷L. Kavan, L. Dunsch, H. Kataura, A. Oshuyama, M. Otani, and S. Okada, *J. Phys. Chem. B* **107**, 7666 (2003).
- ¹⁸J. H. Smet, T. P. E. Broekaert, and C. G. Fonstad, *J. Appl. Phys.* **71**, 2475 (1992).
- ¹⁹M. Tsuchiya, H. Sakaki, and J. Yoshino, *Jpn. J. Appl. Phys., Part 2* **24**, L466 (1985).
- ²⁰J. A. Durães, M. J. Araujo, R. F. Souto, A. Romariz, J. C. da Costa, A. M. Ceschin, and S. G. C. Moreira, *Appl. Phys. Lett.* **89**, 133502 (2006).
- ²¹J. Kong, C. Zhou, E. Yemilmez, and H. J. Dai, *Appl. Phys. Lett.* **77**, 3977 (2000).
- ²²P. L. McEuen, M. Bockrath, D. H. Cobden, Y. G. Yoon, and S. G. Louie, *Phys. Rev. Lett.* **83**, 5098 (1999).
- ²³S. Sanvito, Y. K. Kwon, D. Tomanek, and C. J. Lambert, *Phys. Rev. Lett.* **84**, 1974 (2000).
- ²⁴H. J. Li, W. G. Lu, J. J. Li, X. D. Bai, and C. Z. Gu, *Phys. Rev. Lett.* **95**, 086601 (2005).
- ²⁵M. A. Kastner, *Rev. Mod. Phys.* **64**, 849 (1992).
- ²⁶D. Dubois, K. M. Kadish, S. Flanagan, and L. J. Wilson, *J. Am. Chem. Soc.* **113**, 7773 (1991).
- ²⁷L. Echegoyen and L. E. Echegoyen, *Acc. Chem. Res.* **31**, 593 (1998).
- ²⁸K. M. Kadish and R. S. Ruoff, *Fullerenes: Chemistry, Physics, and Technology* (Wiley, New York, 2000).